Temperature Measurement in Rapid Thermal Processing Using the Acoustic Temperature Sensor

Yong Jin Lee, Butrus T. Khuri-Yakub, and Krishna Saraswat

Abstract—**Acoustic techniques are used to monitor the temperature of silicon wafers in rapid thermal processing environments from room temperature to 1000°C with ±5°C accuracy. Acoustic transducers are mounted at the bases of the quartz pins that support the silicon wafer during processing. An electrical pulse applied across the transducer generates an extensional mode acoustic wave which is guided by the quartz pins. The extensional mode is converted into Lamb waves (a guided plate mode) in the silicon wafer which acts as a plate waveguide. The Lamb wave propagates across the length of the silicon wafer and is converted back into an extensional mode at the other pin. The extensional mode acoustic wave is detected and the total time of flight is obtained. The time of flight of the extensional mode in the quartz pin is measured using pulse echo techniques and is subtracted from the total time of flight. Because the velocity of Lamb waves in the silicon wafer is systematically affected by temperature, the measurement of the time of flight of the Lamb wave provides the accurate temperature of the silicon wafer. The current implementation provides a ±5°C accuracy at 20 Hz data rate. Further improvements in electronics and acoustics should enable ±1°C measurements. The acoustic temperature sensor (ATS) has several advantages over conventional temperature measurement techniques. Unlike pyrometric measurements, ATS measurements are independent of emissivity of the silicon wafer and will operate down to room temperature. ATS also does not have the contact and contamination problems associated with thermocouples.**

I. Introduction

The temperature dependence of Lamb waves (guided plate mode acoustic wave) is used to measure the temperature of the silicon wafer in a rapid thermal processing environment. The key component of the acoustic temperature sensor (ATS) is the efficient excitation and detection of the acoustic wave. Two general methods of acoustic wave generation and detection have been investigated. In one approach, a pulsed laser is used to generate the acoustic wave via the photoacoustic phenomenon and a probe beam deflection is used to detect the wave [1]. Although this solution is elegant as it provides a fully noncontacting method of excitation, the signal to noise (S/N) ratio was found to be inadequate. The alternative method of acoustic wave excitation and detection on the wafer is through its contacts with the support pins. Although this technique relies on a physical contact to transfer acoustic energy, it does not alter the geometry of the wafer placement in the chamber.

Manuscript received October 20, 1993; revised August 20, 1995.

Y. J. Lee was with the Ginzton Laboratory, Stanford University, Stanford, CA 94305 USA. He is now with CVC Products Inc., Fremont, CA 94539 USA.

B. T. Khuri-Yakub is with the Ginzton Laboratory, Stanford University, Stanford, CA 94305 USA.

K. Saraswat is with the Center for Integrated Systems, Stanford University, Stanford, CA 94305 USA.

Publisher Item Identifier S 0894-6507(96)01139-6.

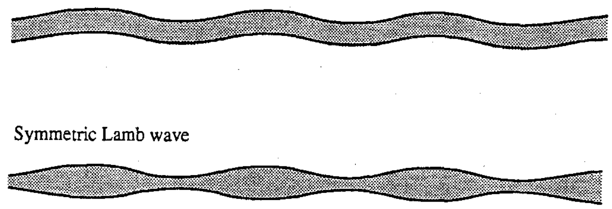

Fig. 1. Zeroth order antisymmetric and symmetric Lamb waves.

The critical aspects of the pin-coupled excitation and detection are: i) repeatability of contact which is controlled by adjusting the contact tip radius and the contact force, ii) compensation for acoustic travel along the quartz rods which is accomplished by measuring the pulse-echo time of flight in the rod, and iii) control of the effects of wafer resonance which is accomplished by adjusting the timing between the acoustic pulses. A practical issue for the installation of the system into a reactive chamber is the isolation of the transducer from the processing environment. The isolation serves to protect the transducers from the harsh reactive conditions and heat in the processing chamber. The isolation also protects the processing environment from possible contamination from the transducer.

II. Temperature Dependence of Lamb Waves

Lamb waves are elastic perturbations propagating along a plate with free boundaries, with displacements occurring both parallel and perpendicular to the direction of wafer propagation [2]–[4]. The two lowest order Lamb waves, the zeroth order symmetric and antisymmetric modes are illustrated in Fig. 1.

Among the various Lamb wave modes that can be generated in the wafer, the zeroth order antisymmetric mode (A0) is dominant in the ATS. The ATS thus relies on the temperature dependence of the A0 mode propagation exclusively. Fig. 2 shows the theoretical Lamb wave group and phase velocities for wave propagation on 500-μm thick (100) intrinsic silicon wafers along the (100) direction [5]. In the ATS, both the group velocity and the phase velocity determine the time of flight.

The theoretical temperature dependence of Lamb waves is obtained from the temperature dependence of the elastic stiffness constants [6]–[8], and the dispersion relation is solved as a function of temperature using the techniques described in

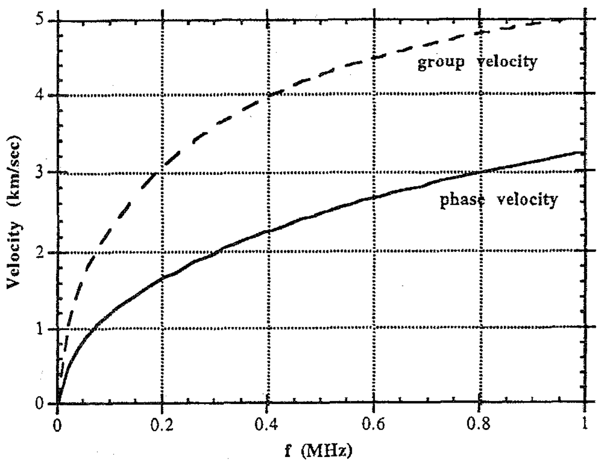

Fig. 2. Zeroth order antisymmetric Lamb wave velocity propagating in a 500 μm (100) intrinsic silicon along the (100) direction.

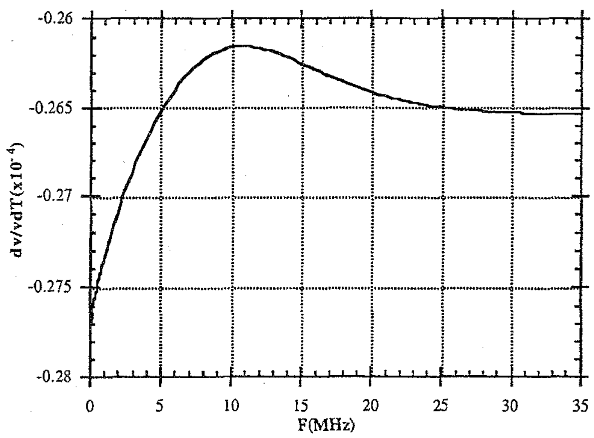

Fig. 3. Relative change in Lamb wave velocity per 1°C change in wafer temperature.

[5]. The relative change in A0 mode Lamb wave velocity as a function of temperature is solved for a range of frequencies (Fig. 3).

III. Principle of Operation

The set up of the ATS is shown in Fig. 4. Lead zirconium titanate (PZT) transducers with a center frequency of 300 kHz are mounted at the bases of the quartz support pins. An electrical pulse applied across a transducer generates an extensional mode acoustic wave in the quartz pin. The acoustic pulse travels up the quartz pin and is converted into Lamb wave in the wafer at the Hertzian contact. The Lamb wave propagates out from the contact point toward the receiver pin at the opposite side of the wafer where it is again converted into an extensional mode in the quartz rod. The wafer is placed so that the acoustic wave propagation is measured along the (100) crystallographic orientation of the wafer. The extensional mode acoustic wave at the opposite pin is detected by the transducer attached at the base of the pin. The time of flight between the pulsing of the excitation transducer

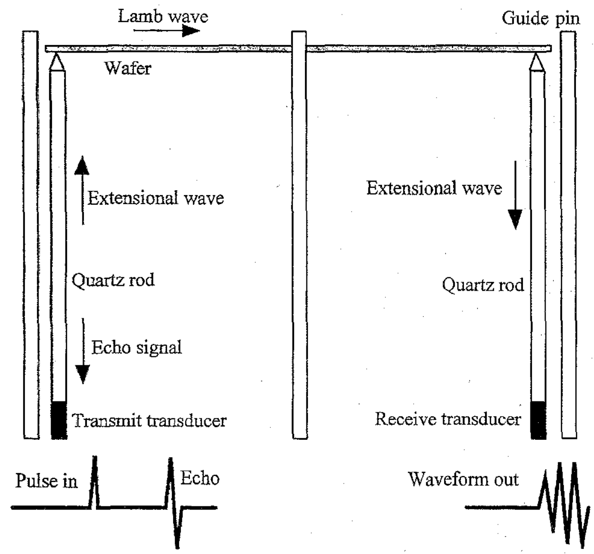

Fig. 4. Set-up for the acoustic temperature sensor (ATS).

and a zero-crossing on the received signal is measured. At the same time, the pulse-echo signal of the acoustic wave propagating up the quartz rod and reflected off the Hertzian contact back into the rod is also measured. The pulse echo signal is effectively subtracted from the total time of flight to obtain the temperature dependent time of flight of the Lamb wave in the wafer.

IV. Measurement Electronics

In terms of electronic implementation, the subtraction can be performed in two ways. In the first method, two separate time delay measurements for the total time of flight and pulse echo are measured, and the pulse echo is subtracted from the total time of flight in a computer. In the second method, a zero crossing on the pulse echo signal is used to start the counter, and a zero crossing on the total time of flight signal is used to stop the counter (Fig. 5). In both methods, the computer uses the measured time of flight data to control the position of the *Enable Counter Start* and *Enable Counter Stop* signals on the time interval counter.

The ATS was implemented using the second technique. The majority of the electronics are standard measurement instruments controlled through the General Purpose Interface Bus (GPIB) as shown in Fig. 6. The computer inputs the initial positions of the *Enable Counter Start* and *Enable Counter Stop* values into the delay generator. The delay generator sends a rising edge signal into a pulser/receiver which sends a pulse to the transducer pin. The pulse echo signal is detected and amplified by the pulse/receiver and the signal is sent to the time interval counter. After the counter has been armed by the *Enable Counter Start* signal, the pulse/echo signal triggers the start of the counter. Roughly 35 μs later, a trailing edge *Enable Counter Stop* signal is sent to the time interval counter. At about the same time, the total time of flight signal is detected at the opposite transducer pin. The signal is amplified using

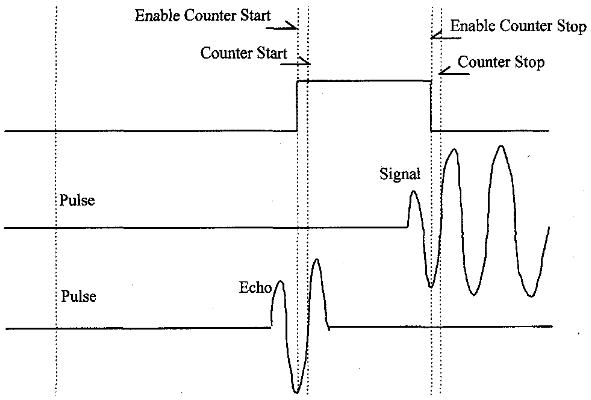

Fig. 5. Timing diagram for deriving time of flight of Lamb wave propagation where the pulse-echo signal is used to start the time interval counter and a specified zero-crossing of the total time of flight signal is used to stop the counter.

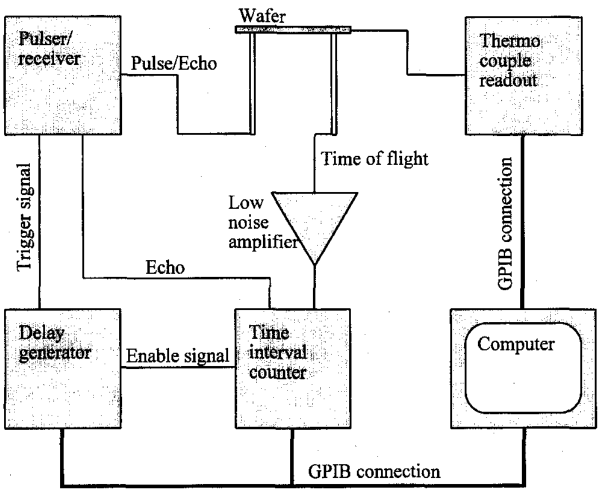

Fig. 6. Block diagram of the time of flight measurement electronics.

a low-noise pre-amplifier, and the signal is used to stop the counter. The time interval counter then sends the effective time of flight of the Lamb wave into the computer through the GPIB bus. The Lamb wave time of flight signal is used to obtain the temperature of the wafer and is also used to update the values of the *Enable Counter Start* and *Enable Counter Stop* signals. A thermocouple monitor is used to record the temperature of the wafer during calibration and some measurement runs.

The repetition rate of the pulse/data acquisition is determined by the decay time of the multiple reflections in the wafer. It has been found experimentally that multiple reflections in the wafer become undetectable about 50 ms after the initial pulsing of the excitation transducer. A data rate (i.e., pulse rate) of 20 Hz is thus used for the ATS.

V. Transducer Pins

Wafers in many rapid thermal processors are supported on quartz pins during processing. The low thermal conductivity of quartz and the small contact area prevents heat transfer from the wafer into the support pins, thus avoiding temperature nonuniformities. The quartz pins used in the acoustic temperature sensor are circular in cross section with a diameter of 1.5 mm and a length of 17.5 cm (Fig. 7). The tips of the pins are sharpened into a point and the top is rounded to a radius of 100 μm. The spherical tip ensures a single, reproducible Hertzian contact with the silicon wafer. Lead zirconium titanate (PZT) 5H is used as the transducer material. The cylindrical PZT has the same radius as the quartz pin and is 4 mm long with the direction of polarization along its length. The ends of the PZT, as well as the flat end of the quartz rod are metalized with gold. Part of the side of the quartz rod at the flat end is also metalized with gold to provide an electrical

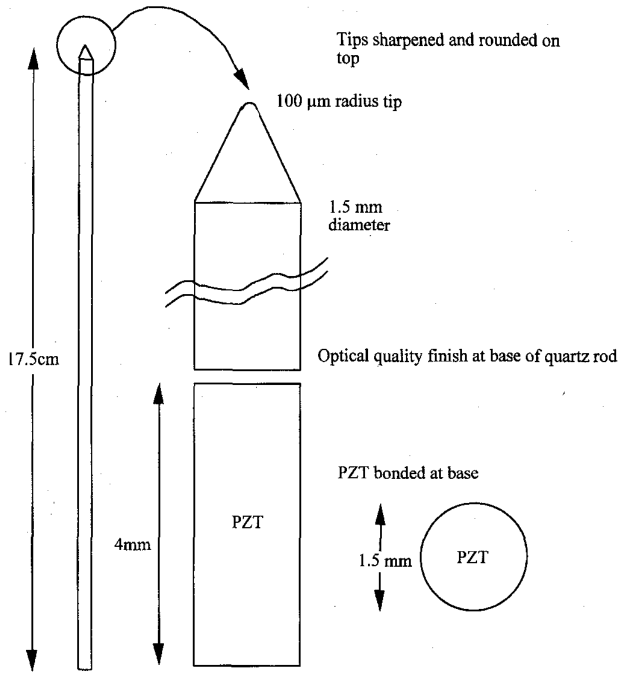

Fig. 7. The transducer pin design for implementation of the ATS.

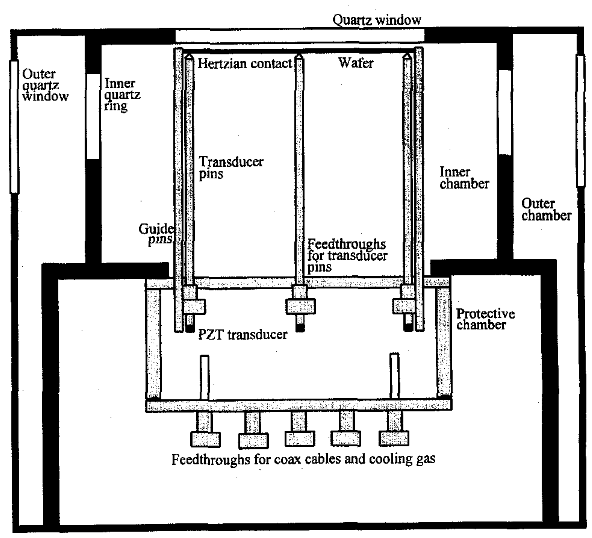

Fig. 8. Implementation of the ATS in a single-zone rapid thermal processor.

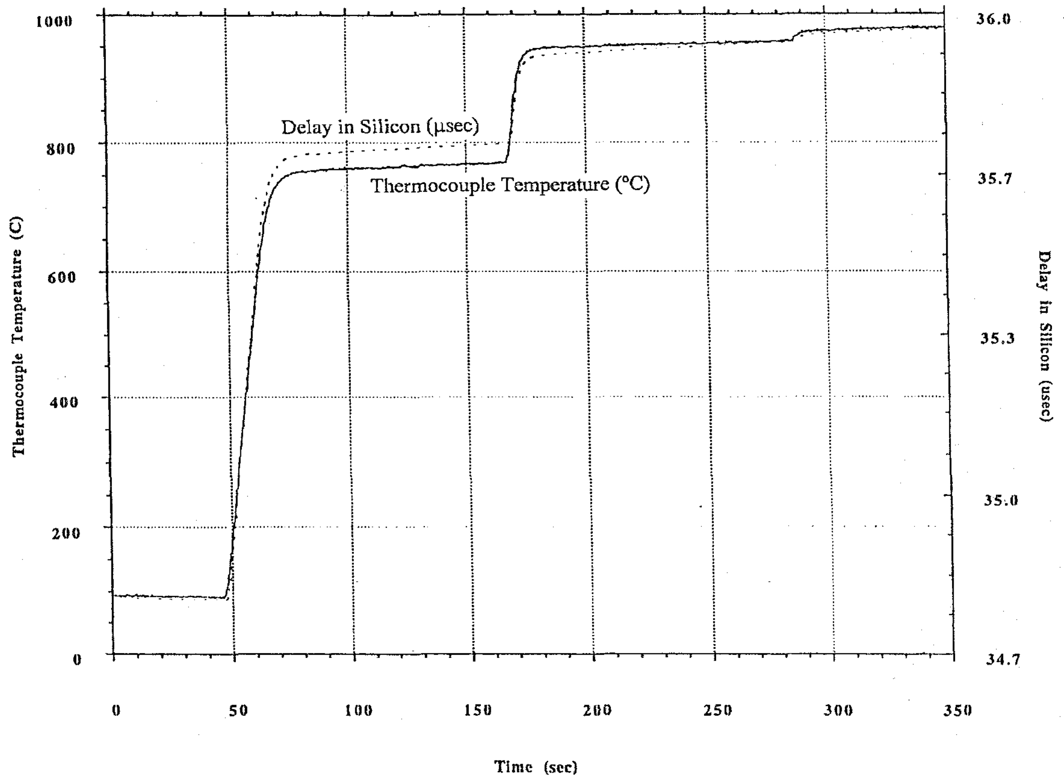

Fig. 9. Calibration run used to obtain a polynomial model for temperature dependence.

contact pad. Besides providing electrical contact to the PZT, the gold metallization at the end of the quartz rod protects the PZT from radiation that is guided by the quartz rod. The high reflectivity of gold ensures that most of the radiation energy is reflected off the quartz-PZT interface. The PZT is attached to the quartz rod using an epoxy bond, and electrical contacts are made at the bottom of the PZT and at the metalized side of the quartz rod. A protective enclosure is attached around the PZT, and low vapor pressure silicon rubber is injected into the enclosure to encapsulate the transducer and the wire bonding pads.

VI. Transducer Module

Three transducer pins, located 120° apart, are housed in a cylindrical chamber and are supported by Viton o-ring feedthroughs (Fig. 8). The exact length of the pins extending out of the transducer housing can be adjusted by loosening the o-rings around the pins and sliding them up or down. The o-ring pressure required to hold vacuum, introduces between 10% and 20% one-way loss in acoustic energy depending on the tightness of the seal. The general waveform, however, remains the same. Care must be taken to ensure that there are no direct contacts between the chamber and the pins in the feedthroughs as it causes significantly larger (>50%) loss in acoustic energy.

A pneumatically operated bellows system brings the transducer housing and inner chamber into a lowered position for manual loading of the wafer. Because the wafer is loaded into the chamber manually, three guide pins extending above the support pins by about 2 mm are needed to guide the user in placing the wafer. During processing, the transducer assembly is raised and the wafer is brought about 3 mm below the top quartz window for efficient heating. The wafer rests freely on the three pins without any clamping mechanism.

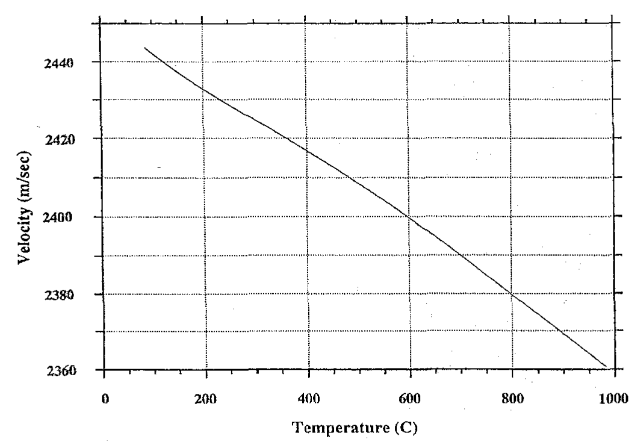

Fig. 10. Regressional model of Lamb wave velocity along the (100) direction as a function of temperature.

The transducer chamber ambient is isolated from the processing ambient to protect the transducers from the harsh reactants and high temperatures. The isolation also prevents the

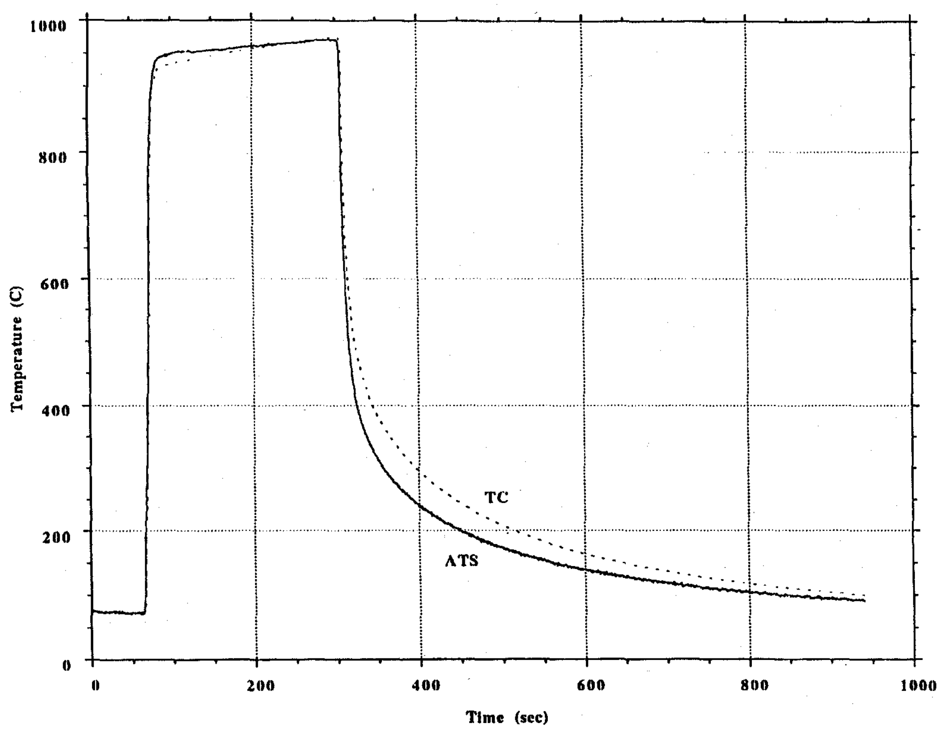

Fig. 11. Comparison of ATS and thermocouple.

contamination of the processing environment by the transducer material. The chamber is made of aluminum due to its ease of machinability. After polishing, the outer surface of the transducer housing was plated with nickel to minimize the absorption of lamp radiation. The bottom of the chamber is removable so that the transducers can be accessed. The bottom cover has vacuum compatible feedthroughs for the coaxial cables, gas lines, and thermocouple probes. The coaxial cables carry the excitation and detection electrical signals. The gas lines allow the flow of nitrogen into the system to regulate the temperature of the chamber ambient. A thermocouple probe is used to monitor the temperature of the ambient.

Excessive flow of nitrogen, while keeping the chamber cool, causes significant turbulence which is picked up as noise by the transducers. A flow setting which maintains the chamber temperature at about 50°C during high temperature runs has been found to be optimal.

VII. Calibration Procedure

A calibration is made with a reference thermocouple that is welded onto the center of the wafer to experimentally determine the temperature dependence of Lamb wave velocity in silicon along the (100) crystallographic direction. Fig. 9 shows the plot of the thermocouple reading and the corresponding time of flight across the wafer (note the time of flight is a nonlinear function of wafer temperature). The calibration is made for steady-state conditions with constant lamp power settings to eliminate the dynamic effects of temperature distribution over the wafer. Lamp power settings at 0%, 20%, 40%, and 60% are used. All excitation and measurement techniques are kept identical to those of actual measurement conditions.

The effect of thermal expansion of the wafer is subsumed in the calibration procedure. As the wafer expands at higher temperatures, the Hertzian contact remains intact and the quartz pins move further apart, increasing the travel distance of the Lamb wave across the wafer. The 0.4% increase in the time of flight caused by the thermal expansion, however, is about an order of magnitude smaller than the 3.5% increase caused by the change in Lamb wave velocity over the same temperature range.

A fourth order polynomial model for the temperature was obtained from regressional analysis of the calibration run shown in Fig. 9. The fourth-order polynomial used to convert velocity data into temperature is given by

$$T = -4138700 + 4479.1v - 1.28967v^2 - 5.8480 \times 10^{-5}v^3 + 4.9016 \times 10^{-8}v^4$$

where T is the temperature, and v is the measured Lamb wave velocity. The model is plotted in Fig. 10. The fit of the data, R, is 0.9998. The calibration run has a data scatter of 8 ns which corresponds to roughly ±3°C error. The effect of the scatter, however, is eliminated by least squares fitting of the data to the fourth order polynomial.

Because the time of flight data is based on measuring a particular zero-crossing within a wave train, both the phase and group velocities are involved in the measurement. The group velocity is involved in carrying the wave train to the general area of detection, while the phase velocity of the waves within

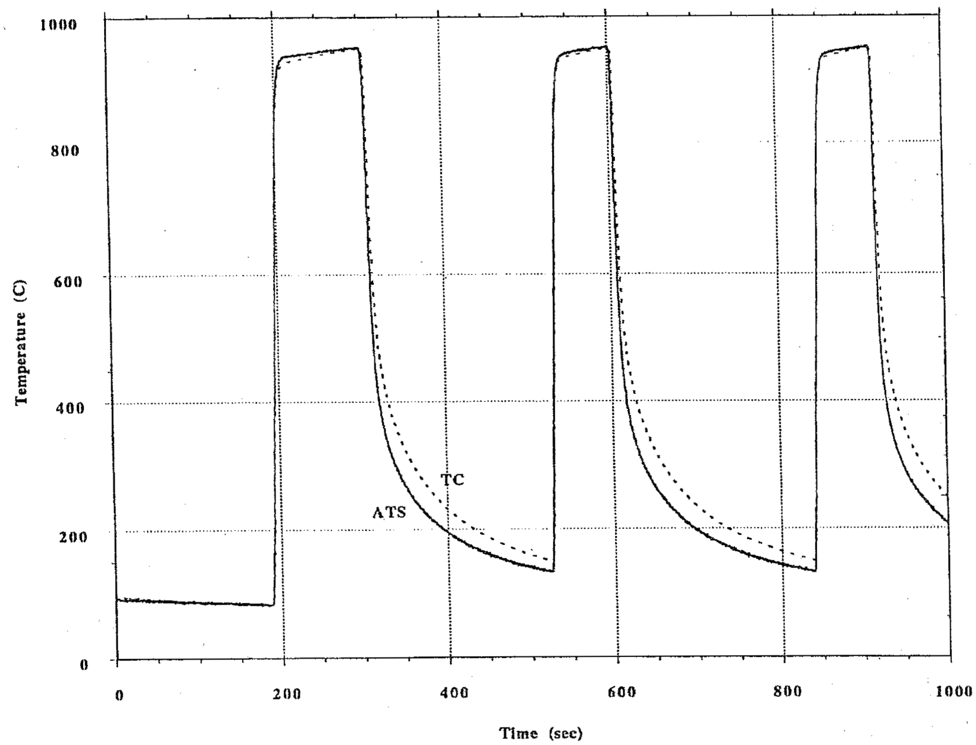

Fig. 12. Repeatability of ATS measurements.

the envelope determines the exact position of the measured zero crossing. The measured velocity value of roughly 2450 m/s at room temperature is between the theoretical phase and group velocities (Fig. 2).

The average relative velocity dependence ($\frac{dv}{vdT}$) obtained experimentally is about $3.8 \times 10^{-6}/°C$. This value is larger than the value of $2.8 \times 10^{-6}/°C$ obtained from extrapolation of McSkimmin's data [6]. The discrepancy is due to the fact that while the theory was performed for phase velocities alone, the experimental value is due to the combined effects of group and phase velocities.

VIII. Experimental Results

The polynomial model (Fig. 10) was applied to a dynamic temperature ramp-up and ramp-down in a rapid thermal processor. Acoustic thermometry requires no thermal mass contacting the wafer and thus has a faster response time than the reference temperature taken with a type-c thermocouple welded onto the wafer. The difference in the ramp-up and ramp-down transients between acoustic and thermocouple measurements, however, is primarily due to the fact that the wafer edges respond faster to temperature control than the wafer center. Due to the triangular position of the transducer pin contact points, the ATS effectively measures the temperature of the wafer off its center point. The acoustic temperature measurement made at a 20 Hz data rate is compared with the thermocouple data in Fig. 11. Repeatability of the data over several temperature ramp-ups and ramp-downs is presented in Fig. 12.

Presently, ATS is capable of measuring temperature with an accuracy of ±5°C (the time of flight measurement error by itself is equivalent to ±3°C). Further improvements in system implementation including improvements in the transducer and front-end electronics design as well as enhancements in numerical signal conditioning, is expected to improve the accuracy to ±1°C.

IX. Conclusion

Temperature dependence of Lamb wave propagation across the silicon wafer has been successfully used to measure the wafer bulk temperature. Because the temperature measurement uses a temperature dependent physical phenomenon confined within the bulk of the wafer, external and boundary conditions (e.g. emissivity and lamp interference) do no affect the measurements. The ATS has been installed into a Texas Instruments-designed rapid thermal processor without altering the geometry of wafer placement on the quartz support pins. Measurements from room temperature to 1000°C has been obtained with ±5°C accuracy.

Acknowledgment

The authors thank M. Moslehi at Texas Instruments for providing helpful suggestions and guidance in the project. C. H. Chou contributed to the theoretical analysis of Lamb waves and the instrument control software. K. H. Chua provided invaluable help in obtaining the calibration and experimental data. L. Booth helped with the installation of the rapid thermal processor into the cleanroom. J. Vhrel and T. Carver fabricated the transducer pins, and F. Nalvarian fabricated the transducer isolation chamber. M. Galt built the low-noise preamplifiers for the transducers. M. Gutierez provided us with the thermocouple wafers.

REFERENCES

[1] Y. J. Lee, C. H. Chou, B. T. Khuri-Yakub, and K. C. Saraswat, "Noninvasive process temperature monitoring using laser-acoustic techniques," in *1990 VLSI Technol. Symp.*, Honolulu, HI, June 5–7, 1990.

[2] M. Redwood, "Mechanical waveguides," *The Propagation of Acoustic and Ultrasonic Waves in Fluids and Solids With Boundaries.* New York: Pergamon, 1960.

[3] B. A. Auld, *Acoustic Fields and Waves in Solids.* New York: Wiley, 1973.

[4] I. A. Victorov, "Raleigh and Lamb waves," *Physical Theory and Applications.* New York: Plenum, 1967.

[5] Y. J. Lee, "Temperature measurement in rapid thermal processors using acoustic techniques," Ph.D. dissertation, Department of Electrical Engineering, Stanford University, Stanford, CA, Feb. 1994.

[6] H. J. McSkimmin, "Measurement of elastic constants at low temperatures by means of ultrasonic waves—Data for silicon and germanium single crystals, and for fused silica," *J. Appl. Phys.*, vol. 24, no. 8, p. 988, 1953.

[7] J. A. Gerber and A. V. Granato, "Theory of the temperature dependence of second-order elastic constants in cubic materials," *Phys. Rev.*, vol. 11, no. 10, p. 3990, 1975.

[8] S. Rajagopalan, "Temperature dependence of the nonlinearity constant and ultrasonic attenuation in pure silicon and germanium," *J. Appl. Phys.*, vol. 54, no. 6, p. 3166, 1983.

Yong Jin Lee received the B.S., M.S., and Ph.D. degrees in electrical engineering from Stanford University, Stanford, CA, where he also received the A.B. degree in economics and the M.S. degree in engineering management.

He is the Director of Equipment and Process Control, CVC Products, Fremont, CA. Before joining CVC Prdoucts, Inc., he was at Texas Instruments, where he was involved in development of sensors, sensor fusion, and process control during the MMST and Process Synthesis programs. His expertise covers sensors, sensor fusion, process control, semiconductor processing, and process synthesis. He is currently the program manager of ARPA-funded NCAICM research program for the development of advanced semiconductor process modules. He has 15 publications and five patents pending or issued.

Dr. Lee was the recipient of the Frederick Terman Award and is a member of Tau Beta Pi and Phi Beta Kappa.

Butrus T. Khuri-Yakub, photograph and biography not available at the time of publication.

Krishna Saraswat, photograph and biography not available at the time of publication.